Multiscale Modelling of Cancer: Micro-, Meso- and Macro-scales of Growth and Spread

Mark A. J. Chaplain

Introduction

Cancer is a complex, dynamic disease with underlying processes occurring over the full range of biological scales from genetic, through proteomic, cellular, tissue, organ, to organism and sometimes even the whole population level. The first detectable (palpable) symptoms are almost always macroscopic, but mechanisms are also present *a priori* at the cellular level and these in turn originate from changes/mutations in the individual's DNA. Perhaps one of the most difficult questions of modern medicine is how to intervene and manipulate the complex system of the patient's body to affect changes in dynamics which can bring it back from a state of disease to either full remission or stabilisation. Given the complexity of the system a chance to answer that question should be sought by complementing the traditional clinical methods with mathematical and computational modelling and simulations. However, while developing predictive models one of the most important key aspect of the disease to be considered, if not the key aspect, is its multi-scale character.

In one of the most influential cancer papers of the last two decades, Hanahan and Weinberg [26] defined what they termed to be the six hallmarks of cancer: (i) sustaining proliferative signalling; (ii) evading growth suppressors; (iii) activating invasion and metastasis; (iv) enabling replicative immortality; (v) inducing angiogenesis; (vi) resisting cell death. More recently the authors [27] updated this list to also include two other emerging hallmarks: (i) deregulating cellular energetics; (ii) avoiding immune destruction, and two enabling characteristics (i) genome instability and mutation; and (ii) tumour promoting inflammation. These hallmarks are linked with phenotypic traits that give cancer cells an evolutionary advantage over healthy cells. Furthermore, in [27] Hanahan and Weinberg described four main types

M. A. J. Chaplain (✉)
School of Mathematics and Statistics, University of St Andrews, St Andrews, Scotland
e-mail: majc@st-andrews.ac.uk

M. Bizzarri (ed.), *Approaching Complex Diseases*, Human Perspectives in Health Sciences and Technology 2, https://doi.org/10.1007/978-3-030-32857-3_7

of intracellular circuit (signal transduction pathway) regulating the operation of cells: (i) proliferation circuits; (ii) viability circuits; (iii) motility circuits; and (iv) cytostasis and differentiation circuits. The failure or dysregulation of these four circuits jointly make up the characteristic phenotype of cancer cells, corresponding directly with four of the hallmarks given above. In contrast to healthy cells that carefully control the production of specific growth and proliferative signals, cancer cells have an abnormal progression through the cell cycle and divide rapidly. Equally they have much higher viability compared to normal cells; resisting cell death, avoiding immune destruction, genome instability and mutation make cancer cells somewhat "immortal". The outcome is the formation of macroscopic structures such as solid tumours that can be observed clinically. Despite enormous progress full understanding of these processes is difficult because we are dealing with a complex interplay between various subprocesses occurring with different dynamics at different spatial scales.

One of the most dangerous properties of malignant tumours is their ability to invade surrounding tissues and to metastasize. The invasion or infiltration of surrounding tissue by cancer cells can impair the tissue or organ function. However, a more dangerous aspect of invasion is the infiltration of blood and lymph vessels. When cancer cells penetrate the vessel lumen they may migrate with blood or lymph to distant sites in the body to form new tumours, i.e. metastases. It is worth mentioning that angiogenesis also contributes; through the formation of new blood vessels within the tumour it facilitates the migration of tumour cells. Metastasis of cancer makes patient's treatment very difficult. It prevents the effective resection of the primary tumour, as new outbreaks cause recurrence of the disease. There are many mechanisms that enable cancer cells invasion and metastasis, together making the motility circuit. One can mention here the frequently occurring over-expression of genes encoding extracellular matrix-degrading enzymes such as matrix metalloproteinases (MMPs). However, perhaps the most characteristic change is the loss of the functionality of the protein E-cadherin, which is the main molecule responsible for binding between epithelial cells.

While it is clear that there are many different, inter-connected temporal and spatial scales that are important during the development of any tumour, within these there are three clearly demarcated "fundamental scales" linked to each other which, when considered together, go to make up understanding the complex phenomenon that is cancer: the intra-cellular scale, the cellular scale and the tissue scale. At the level of intracellular processes we must include within the description complicated but essential phenomena such as signal transduction cascades, gene regulatory networks or cell cycle regulation. Doing so aids our understanding of the differences at the intracellular level between normal and transformed cells and therefore improves the efficiency of anti-cancer cell-cycle-dependent drugs. Another challenge while modelling intracellular processes is to understand how the three-dimensional structure of DNA and chromatin affects gene expression within signalling pathways crucial for the disease development. Although it is known that cancer

is most often caused by the accumulation of mutations in genes involved in cell cycle regulation and apoptosis, another important issue is how the disease progression is influenced by structural or epigenetic changes within the cell nucleus.

At the level of cellular colonies and tissue there are two main approaches towards modelling complex biological processes like cancer: continuum and discrete. Continuum methods, that are derived from principles of continuum mechanics, have proved to be very useful in modelling phenomena at the tissue scale such as general tumour growth. However, one of the main drawbacks of continuum modelling is the difficulty in representing individual cell properties. Including these and intracellular processes in multi-scale phenomena such as cancer is becoming more and more important as experimental data across multiple scales becomes available. Alternative approaches rely on an individual-based description of a single cell. The main advantage of such methods is related to the relative simplicity of transmitting detailed biological processes into dynamics and development of cell populations and tissue. The main disadvantage is the computational cost which increases rapidly with the number of simulated cells. However the problem of high computational complexity can be addressed by selecting appropriate algorithms and by efficient implementation on high performance computing (HPC) systems.

Further milestones related to cancer modelling will be adapting the models for specific cancer types and specific patients. The latter means not only the acquisition of biochemical parameters but also the acquisition of medical image data for individual patients. This will be a definite step towards personalised medicine, which has a chance to completely reform our approach to the patient and his treatment. Already today imaging studies are of great importance in diagnosis and planning surgical procedures. However, especially for treatment of non-resectable tumours, such imaging studies could also be important in selecting the appropriate treatment or monitoring the disease dynamics.

In this chapter we provide a brief overview of current cancer modelling ("multi-scale mathematical oncology") at the three different scales previously mentioned – intra-cellular, cellular and tissue – drawing on recent work by Sturrock et al. [49, 50], Szymańska et al. [51] and Domschke et al. [15]. In Sect. 2 we discuss the modelling of intracellular dynamics, specifically gene regulatory networks (GRNs). In particular we focus on the canonical transcription factor – Hes1. In Sect. 3 we focus on the cell scale, in particular investigating cell-cell/cell-matrix dynamics using an individual-based (or agent based) force-based model. In Sect. 4 we model cancer cell invasion at the tissue or macroscale using a system of nonlinear, nonlocal partial differential equations. This system explicitly accounts for cell-cell adhesion and also cell-matrix adhesion through a non-local term developed originally by Armstrong et al. [7] and then originally applied to cancer invasion modelling by Gerisch and Chaplain [19]. In the final Discussion Sect. 5, we provide directions for future research by combining modelling at all scales and highlight recent work on modelling cancer treatment (chemotherapy and radiotherapy) and the metastatic spread of cancer.

The Microscale: Gene Regulatory Networks and Transcription Factors

At the heart of cellular function and communication lies segments of DNA (genes) and their associated gene regulatory networks (GRNs). A GRN can be defined as a collection of genes in a cell which interact with each other indirectly through their RNA and protein products. GRNs are vital to intracellular signal transduction and indirectly control many important cellular functions such as cell division, apoptosis and adhesion. One specific class of GRN involves proteins called transcription factors, which alter the transcription rate of genes in response to intra- or extracellular cues. Transcription factors may reduce or increase the transcription rate of a given gene, respectively inhibiting or promoting its production. If the inhibition (or promotion) is directed towards the transcription factor's own gene, either directly or indirectly, there is negative (or positive) feedback. Negative feedback loops are an important component of many gene networks and are found within a wide range of biological processes e.g. inflammation, meiosis, apoptosis and the heat shock response [32]. Mechanically speaking, systems which contain negative feedback should (and in fact are known to) exhibit oscillations in the levels of the molecules involved. Furthermore, in many biological processes, it is the oscillatory expression which is of particular importance.

Mathematical modelling of GRNs began some 50 years ago with the papers of [21, 23], in which a negative feedback model for a simple, single mRNA-protein feedback system was proposed. However, while GRNs are known to exhibit periodic fluctuations in mRNA and protein concentrations (e.g. the results for the Hes1 system, cf. [29]), these early models, which were restricted to purely temporal ODEs, could not produce oscillatory behaviour. Subsequently, discrete delay ODE models were proposed, which although reproducing the oscillatory dynamics, neglect the spatial structure of the cell (nucleus/cytoplasm). The first spatial models (for theoretical intracellular systems) were proposed in the 1970s by Glass and co-workers [20, 47] and similarly in the 1980s by Mahaffy and co-workers [8, 36, 37]. The inclusion of spatial terms (rather than, for example, a delay in a system of ODEs) is capable of producing the experimentally observed oscillations [31, 33–35, 49, 50, 52]. Moreover, in addition to the computational results of the previous papers, the work of Chaplain et al. [9] has rigorously proved, for the Hes1 system, that molecular diffusion causes oscillations.

The Hes1 System

The Hes1 protein may be viewed as the simplest transcription factor i.e. the Hes1 protein downregulates its own hes1 mRNA production, making it the canonical negative feedback system. This system (as well as the more complex p53-Mdmd2 system) was considered as a spatial problem in [49, 50]. Figure 1 shows a schematic

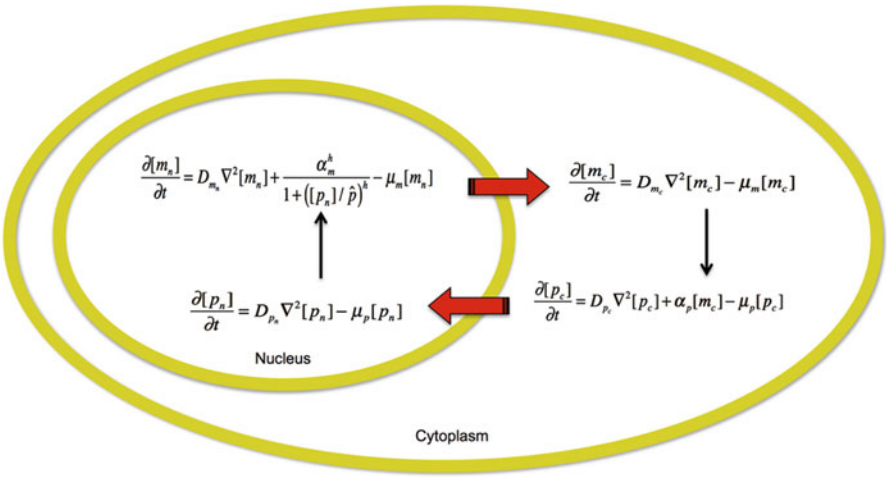

Fig. 1 Schematic diagram showing the Hes1 gene regulatory network. Hes1 protein is produced in the cytoplasm (translation), diffuses through the cytoplasm, across the nuclear membrane and into the nucleus where it down-regulates hes1 mRNA. The hes1 mRNA is produced in the nucleus (transcription), diffuses, crosses the nuclear membrane into the cytoplasm and is then translated into Hes1 protein. The equations show the reaction-diffusion events for each molecule and the red arrows denoted passage across the nuclear membrane

diagram of the Hes1 system, with Hes1 protein being produced in the cytoplasm (protein synthesis or translation), diffusing through the cytoplasm, across the nuclear membrane and into the nucleus where it down-regulates hes1 mRNA production (transcription). The hes1 mRNA itself can then diffuse to the nuclear membrane, move across the membrane and into the cytoplasm where it diffuses and is translated in to Hes1 protein in the ribosomes (translation).

These processes of molecular diffusion, protein production (translation) and mRNA production (transcription), along with the downregulation of mRNA can be modelled by the system of PDEs (where $m(\mathbf{x}, t)$, $p(\mathbf{x}, t)$ are the concentrations of hes1 mRNA and Hes1 protein respectively, with subscript n denoting the nucleus, and subscript c denoting the cytoplasm) as follows:

$$\frac{\partial[m_n]}{\partial t} = D_{m_n}\nabla^2[m_n] + \underbrace{\frac{\alpha_m}{1+([p_n]/\widehat{p})^h}}_{transcription} - \mu_m[m_n], \tag{1}$$

$$\frac{\partial[m_c]}{\partial t} = D_{m_c}\nabla^2[m_c] - \mu_m[m_c], \tag{2}$$

$$\frac{\partial [p_c]}{\partial t} = D_{p_c} \nabla^2 [p_c] + \underbrace{\alpha_p [m_c]}_{synthesis} - \mu_p [p_c], \tag{3}$$

$$\frac{\partial [p_n]}{\partial t} = D_{p_n} \nabla^2 [p_n] - \mu_p [p_n], \tag{4}$$

along with zero-flux boundary conditions at the cell membrane and continuity of flux boundary conditions across the nuclear membrane (cf. Fig. 1). Appropriate initial conditions for each molecular species closes the system mathematically. Full details are provided in [49, 50]. Figure 2 shows the results of a computational simulation of the above model in a domain similar to that shown schematically in Fig. 1. The oscillations in both hes1 mRNA and Hes1 protein in both the nucleus and the cytoplasm are clearly seen.

The computational results obtained in [49, 50] indicate that the molecular diffusion plays a major role in generating and controlling the oscillations. This numerical observation was complemented by a full analysis of a 1-dimensional caricature model of the system in [9]. A (nondimensionalised) one dimensional gene regulatory network model (i.e. a caricature of the Hes1 system) was considered on a 1-dimensional spatial domain shown in Fig. 3, with governing equations given by:

$$\frac{\partial m}{\partial t} = D \frac{\partial^2 m}{\partial x^2} + \alpha_m f(p) \delta^{\varepsilon}_{x_M}(x) - \mu m \qquad \text{in } (0,T) \times (0,1), \tag{5}$$

$$\frac{\partial p}{\partial t} = D \frac{\partial^2 p}{\partial x^2} + \alpha_p g(x) m - \mu p \qquad \text{in } (0,T) \times (0,1), \tag{6}$$

with boundary and initial conditions:

$$\frac{\partial m(t,0)}{\partial x} = \frac{\partial m(t,1)}{\partial x} = 0, \qquad \frac{\partial p(t,0)}{\partial x} = \frac{\partial p(t,1)}{\partial x} = 0 \qquad \text{in } (0,T),$$
$$m(0,x) = m_0(x), \qquad p(0,x) = p_0(x) \qquad \text{in } (0,1),$$

where D, α_m, α_p, μ_m and μ_p are positive constants (the diffusion coefficient, transcription rate, translation rate and decay rates of hes1 mRNA and Hes1 protein respectively). Full details can be found in the papers of Sturrock et al. [49, 50] and [9]. Here l denotes the position of the nuclear membrane and therefore the domain is partitioned into two distinct regions, $(0, l)$ the cell nucleus and $(l, 1)$ the cell cytoplasm, for some $l \in (0, 1)$. The point $x_M \in (0, l)$ is the position of the centre of the gene site and by $\delta^{\varepsilon}_{x_M}$ we denote the Dirac approximation of the δ-distribution located at x_M, with $\varepsilon > 0$ a small parameter and $\delta^{\varepsilon}_{x_M}$ has compact support (cf. Fig. 3).

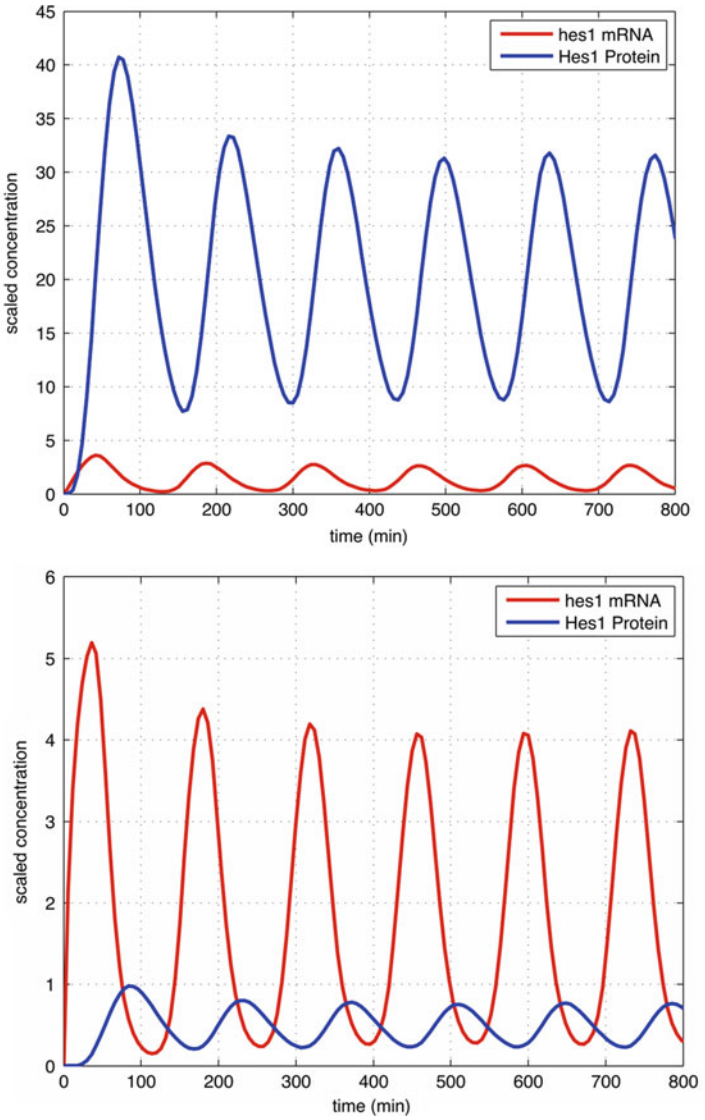

Fig. 2 Plots showing the oscillations in both molecular species (hes1 mRNA, Hes1 protein) in both the nucleus and the cytoplasm

Fig. 3 1-dimensional spatial domain for the caricature Hes1 model. The blue region denotes the nucleus (0,l), while the green region denotes the cytoplasm (l,1). The location x_M (red circle) denotes the location of the gene site where the Hes1 protein binds and down-regulates hes1 mRNA

The nonlinear reaction term $f : \mathbb{R} \to \mathbb{R}$ is a Hill function $f(p) = 1/(1 + p^h)$, with $h \geq 2$, modelling the suppression of mRNA production by the protein (negative feedback). The function g is a step function given by

$$g(x) = \begin{cases} 0, \text{if } x < l, \\ 1, \text{if } x \geq l, \end{cases}$$

since the process of translation only occurs in the cytoplasm.

Chaplain et al. [9] proved rigorously that the diffusion coefficient of the molecules acts as a Hopf bifurcation parameter, therefore showing that molecular movement alone is sufficient to generate the (spatio-temporal) oscillations i.e. space influences time. The two main theorems in the paper are as follows:

Theorem 1 *There exist two critical values of the parameter D, i.e.* D_1^c *and* D_2^c *for which a Hopf bifurcation occurs in the model* (5), (6).

Theorem 2 *At both critical values of the bifurcation parameter* D_1^c *and* D_2^c *a supercritical Hopf bifurcation occurs in the system* (5), (6) *and the families of periodic orbits bifurcating from the stationary solution at each Hopf bifurcation point are stable*.

Further investigation of the importance of spatial aspects in GRNs has examined the Hes1 system both spatially and stochastically [48]. In this paper, a continuous-time discrete-space Markov process approach is used to model the reaction-diffusion kinetics. Since cell populations are naturally heterogenous, a stochastic description with spatial aspects built in allows us to incorporate a variety of differences and to look for emergent behaviour. The approach of [48] can be applied to model other natural pathways or synthetic GRNs cf. the work of Macnamara et al. [33–35], in particular key molecules known to play an important role in cell-cycle control and apoptosis and the inflammatory response *viz.* p53-Mdm2 and NF-κB.

The Mesoscale: Force-Based Individual-Based Modelling of Cell-Cell and Cell-Matrix Interactions

While the model of the previous section highlighted (stochastic) spatio-temporal models of intracellular pathways, in this section, we will focus on a model of cancer growth at the individual cell level developed by Szymańska et al. [51]. There are now a number of different individual-based modelling approaches that one can adopt cf. cellular automata, Cellular Potts Model, hybrid discrete-continuum [1, 5, 6, 14]. Here we adopt an individual-based, force-based model of cell growth which is driven by forces acting upon the cell, and is based upon the model of [42]. More recently this approach has been extended and implemented on a massively parallel system (IBM Blue Gene/Q system) allowing hybrid high performance simulations to describe, for example, tumour growth in its early clinical stage. Details of the

implementation can be found in [11–13]. Adopting this approach, each cell is modelled as an isotropic elastic object capable of migration and division and parameterise it by cell-kinetic, biophysical and cell-biological parameters that can be experimentally measured, from both *in vitro* and *in vivo* experiments [10, 24, 30, 39, 40, 43, 45, 46, 54]. We assume that an individual cell ci in isolation is spherical and characterise the cell shape by its radius R. The position of the cell in 3D space is described by the Cartesian coordinates $(x_{c_i}, y_{c_i}, z_{c_i})$ of its centre.

Regarding cell kinetics, we assume that the cell-cycle is divided into four phases, i.e. mitosis – M-phase, followed by G1-, S-, and G2-phases, after which mitosis occurs again. During a complete cell-cycle, the cell must accurately duplicate its DNA once during S-phase and distribute an identical set of chromosomes equally to two progeny cells during M-phase. M-phase consists of two major events: the division of the nucleus called mitosis and subsequent cytoplasmic division called cytokinesis. G1-phase is an interval between mitosis and the initiation of nuclear DNA replication. It provides additional time for a cell to grow and to replicate its cytoplasmic organelles. G2-phase is again an interval between the completion of nuclear DNA replication and mitosis. Over the course of both the G1- and G2-phases, the cell checks the internal and external environment to ensure that the conditions are suitable and complete preparation for entry into either S-phase or M-phase. When DNA is damaged cell cycle is arrested in G1 or G2 so that the cell can repair DNA damages prior to its duplication or before cell division.

Cell cycle events must occur in a precise order, which should be maintained, even when one of the steps takes longer than usual. For instance, this means that cell division cannot start before DNA replication is complete. Similarly, when DNA is damaged the cell cycle is arrested so that the cell can repair the damage. This is possible because the cell is equipped with molecular mechanisms that can stop the cycle at various checkpoints. Two main checkpoints are located within the G1- and G2-phases. The G1 checkpoint allows the cell to check whether its environment is conducive to divisions and whether its DNA is damaged. If environmental conditions make cell division impossible, instead of entering S-phase a cell can enter a resting state – G0-phase, where it remains until conditions improve and it continues the cell cycle. The G2 checkpoint ensures that the cell has no DNA damage, and DNA replication will be completed before the beginning of mitosis [2].

Interactions between cells are modelled by taking into account the repulsive and attractive forces between cells. Upon compression, i.e. with decreasing distance $d_{c_i c_j}$ between the centres of two adjacent cells, c_i and c_j, of radii, r_{c_i} and r_{c_j}, both their surface contact area and the number of adhesive contacts increase, resulting in an attractive interaction. We assume that adhesive forces are proportional to ρ_m, which is the density of the surface adhesion molecules in the contact zone (which we assume is given for particular cell type), k_B, which is the Boltzmann constant, T, which denotes temperature and $D_{c_i c_j}$, which measures the contact between cells c_i and c_j and is calculated as the volume of the common area of intersecting spheres representing those cells. Experiments suggest that cells only have a small compressibility – the Poisson numbers are close to 0.5, [3, 38]. In this instance,

both the limited deformability and the limited compressibility give rise to a repulsive interaction. Repulsive forces are inversely proportional to the term E_{c_i,c_j}, which is calculated form Young moduli, E_{c_i} and E_{c_j}, and Poisson ratios, v_{c_i} and v_{c_j}. The precise formula is given by:

$$E_{c_i,c_j} = \frac{3}{4}\left(\frac{1-v_{c_i}^2}{E_{c_i}} + \frac{1-v_{c_j}^2}{E_{c_j}}\right). \tag{7}$$

We model the combination of the repulsive and attractive energy contributions by a modified Hertz-model [18, 44] which has the advantage that both the interaction energy and the force can be represented as an analytical expression [16]. Inertia terms are neglected due to the high friction of cells with their environment, and we also do not consider the existence of any memory term as in [18].

$$V_{c_ic_j} = \underbrace{\left(r_{c_i} + r_{c_j} - d_{c_ic_j}\right)^{\frac{5}{2}} \frac{1}{5E_{c_ic_j}} \sqrt{\frac{r_{c_i} r_{c_j}}{r_{c_i} + r_{c_j}}}}_{\text{repulsive interactions}} + \underbrace{\rho_m D_{c_ic_j} 25 k_B T}_{\text{adhesion}}. \tag{8}$$

Cells require access to oxygen from the circulatory system in order to grow and survive. It is well known that cancer cells grow preferentially around blood vessels. Those tumour cells that are located more than about 0.2 mm away from blood vessels were found to be quiescent, while others even farther away were found to be necrotic. This threshold of approximately 0.2 mm represents the distance that oxygen can effectively diffuse through living tissue [53]. Because of the low redox potential and high activation energy that occurs in living organisms, reactions involving molecular oxygen occur only in mitochondria. Therefore, we assume that the loss of oxygen in the tissue takes place only due to its consumption by the cells. The general equation governing the external oxygen concentration $Q(\mathbf{x}, t)$ in the cells' environment may be written:

$$\frac{\partial}{\partial t} Q(\mathbf{x}, t) = D_Q \nabla^2 Q(\mathbf{x}, t) - G(\mathbf{x}, t) + H(\mathbf{x}, t), \tag{9}$$

where D_Q, is the oxygen diffusion coefficient. The function $G(\mathbf{x}, t)$ models the oxygen uptake by cells and the function $H(\mathbf{x}, t)$ models the production of oxygen by vessels. Both of these functions are computed in each time step of the simulation from the current spatial organisation of cells and vessels through interpolation. The force associated with a given cell, c_i, is then given by the expression:

$$F_{c_i} = \underbrace{\nabla V_{c_i}}_{\text{inter-cellular interactions}} + \underbrace{\lambda \nabla Q(x,t)}_{\text{chemotaxis}} \tag{10}$$

where λ is a measure of a cell's chemotactic sensitivity to the oxygen concentration and V_{c_i} is given by

$$V_{c_i} = \sum_{c_j \in B_{\epsilon_{c_i}}} V_{c_i c_j} \tag{11}$$

with $B_{\in_{c_i}}(c_i)$ a sphere (i.e. a ball in $\mathbb{R}^3$) centred on $(x_{c_i}, y_{c_i}, z_{c_i})$, radius $\in_{c_i}$, denoting the maximum inter-cellular interaction region.

Summing all the forces between the cells and assuming a frictional force/drag force proportional to a cell's velocity and then applying Newton's Second Law of motion allows us to integrate a Langevin-type equation to give the spatial location of the cells over time. The direct use of equations of motion for the cells permits one to include more easily the limiting case of very small (or no) noise and is more intuitive. In this approach cells move under the influence of forces and a random contribution to the locomotion which results from the local exploration of space.

Solving the oxygen concentration (which is a global field) together with the individual-based particle system of up to 10^9 cells is a challenging task in the context of parallel processing. First of all, it requires the use of appropriate data structures to optimize the computations of interactions between lattice-free cells. In our approach, the main data structure that stores information about cells is an octal tree. We assume that the domain of simulation is a 3D cube. The cells are arranged in a tree based on the position of their centers. The tree is built recursively starting from the whole domain of simulation, which corresponds to the root of the tree. Subsequently, the cubes are divided recursively into 8 equal cubes with edges reduced by a factor of a half. This procedure is repeated until in the cube under consideration there is only one cell centre. Full details are provided in [51].

Model Application

Figures 4 and 5 show the results of applying the individual-based model to the scenario of a solid tumour (a tumour cord) growing around a central blood vessel

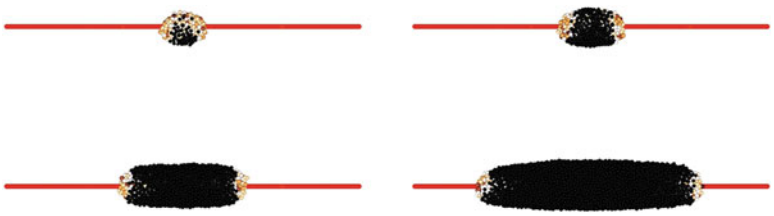

Fig. 4 Plot showing the growing tumour cord around a central blood vessel at times 300, 400, 700 and 1300 h. As the tumour cord grows, cells further away from the vessel become necrotic (black). At the final time of 1300 h, there is a total of around 10,000 cells

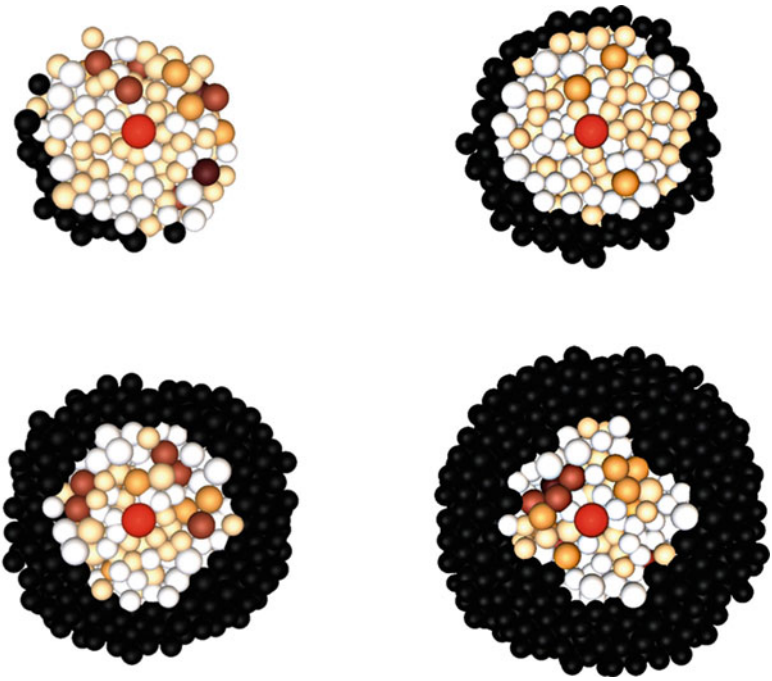

Fig. 5 Plot showing cross-sections of the growing tumour cord around a central blood vessel at times 300, 400, 700 and 1300 h. As the tumour cord grows, cells further away from the vessel become necrotic (black). At the final time of 1300 h, there is a total of around 10,000 cells

which supplies oxygen to the surrounding tissue and cancer cells. The figures show the development of the tumour cord over time and the formation of necrotic (dead) cells towards the outer boundary of the cord, since these are furthest from the blood vessel and the source of oxygen. More detailed simulations can be found in [51], while applications of the approach to avascular solid tumours can be found in Cytowski and Szymańska [11–13].

The Macroscale: Cancer Invasion and Metastasis

This section considers a macroscale model of cancer invasion based focusing on the role of cancer cell adhesion – both cell-cell and cell-matrix. The underlying basis for the model was developed by Armstrong et al. [7] who considered a model for cell sorting, and then developed by Gerisch and Chaplain in [19] as a model for cancer invasion. This approach was further developed more recently by Domschke et al [15] and it is this model that we present here. The variables in the model are cancer cells (density $c(t, x)$), extracellular matrix, ECM, (density $v(t, x)$) and matrix degrading

enzymes, MDE, (concentration $m(t, x)$). The model considers several populations of cancer cells $c_1(t, x)$, $c_2(t, x) \ldots c_n(t, x)$ which are written $\mathbf{c} = (c_1, c_2, \ldots c_n)^{\mathrm{T}}$.

The evolution of the cancer cell sub-population densities is driven by cell random motility, cell-cell and cell-matrix adhesion-mediated directed migration, proliferation, and mutations between the cancer cell sub-populations. This can be expressed as

$$\frac{\partial \mathbf{c}}{\partial t} = \nabla \cdot [\mathbf{D}\nabla \mathbf{c} - \mathrm{diag}(\mathbf{c})\mathcal{A}(t, x, \mathbf{u}(t, \cdot))] + P(t, \mathbf{u})\mathbf{c} + \mathbf{M}(\mathbf{u})\mathbf{c}. \tag{12}$$

Here, the diagonal matrix $\mathbf{D} = \mathrm{diag}(D_{1,1}, \ldots, D_{1,n}) \in \mathbb{R}^{n,n}$ contains the random motility coefficients $D_{1,\mathrm{i}} > 0$ of the cancer cell sub-populations. In this work we assume that those are constants.

Adhesion-mediated directed cancer cell migration is represented using the non-local operator

$$\mathcal{A}(t, x, \mathbf{u}(t, \cdot)) := \begin{bmatrix} \mathcal{A}_1(t, x, \mathbf{u}(t, \cdot))^{\top} \\ \mathcal{A}_2(t, x, \mathbf{u}(t, \cdot))^{\top} \\ \vdots \\ \mathcal{A}_n(t, x, \mathbf{u}(t, \cdot))^{\top} \end{bmatrix} \in \mathbb{R}^{n,p}$$

which maps (t, x) together with the space-dependent function $\mathbf{u}(t, \cdot)$, that is $\mathbf{c}(t, \cdot)$ and $\mathrm{v}(t, \cdot)$, to an $n \times p$ matrix depending on (t, x). Row i in that matrix, i.e. $\mathcal{A}_i\,(t, x, \mathbf{u}(t, \cdot))^T$, represents the velocity of directed cancer cell migration of sub-population i which is induced by cell-cell and cell-matrix adhesion properties of cancer cells and ECM. Here cell-cell adhesion refers to adhesion between cells of sub-population i itself, *self-adhesion*, as well as between cells of sub-population i and sub-population $j \neq i$, *cross-adhesion*. The velocity for sub-population i is defined by the following vector-valued integral, cf. [7] or [19],

$$\mathcal{A}_i(t, x, \mathbf{u}(t, \cdot)) = \frac{1}{R} \int_{B(0,R)} \mathrm{n}(y) \cdot \Omega_i\big(\|y\|_2\big) \cdot g_i(t, \mathbf{u}(t, x + y))\, \mathrm{d}y. \tag{13a}$$

Here, $R > 0$ is the *sensing radius*, $B(0, R) \subset \mathbb{R}^p$ is the ball of radius R centred at zero, and for $x \in \mathrm{d}$ the set $x + B(0, R)$ is the *sensing region* at x. Note that for points $x \in \mathrm{d}$, which are so close to the boundary of d such that $x + B\,(0, R) \cap d) \not\subset d$, the integral in Eq. (13a) is not yet well-defined; we resolve this issue when discussing the boundary conditions for our model in the end of this section. For $y \in B(0, R)$, the unit vector pointing from x to $x + \mathrm{y}$, is denoted by $\mathrm{n}(y)$, i.e.

$$n(y) := \begin{cases} y/\|y\|_2 & \text{if } y \neq 0 \\ 0 \in \mathbb{R}^p & \text{otherwise} \end{cases}. \tag{13b}$$

Furthermore, $\Omega_i(r)$, with $r = \|y\|_2$, is the *radial dependency function* for sub-population i. It characterizes the relative importance of points at distance r from x for adhesion-mediated cell migration. This function is non-negative and normalised such that

$$1 = \int_{B(0,R)} \Omega_i\big(\|y\|_2\big)\,\mathrm{d}\,y. \tag{13c}$$

Finally, the function $g_i(t, \mathbf{u})$ is the i-th component of

$$\mathbf{g}(t, \mathbf{u}) \equiv \mathbf{g}(t, \mathbf{c}, v) = [\mathbf{S_{cc}}(t)\mathbf{c} + \mathbf{S_{cv}}(t)\mathbf{1}v] \cdot (1 - \rho(\mathbf{u}))^+. \tag{13d}$$

In the above, $\mathbf{1} \in \mathbb{R}^n$ is the all-one vector, $\mathbf{Scv}(t) \in \mathbb{R}^{n,n}$ is the diagonal matrix containing the non-negative cell-matrix adhesion coefficients of all cancer cell sub-populations with the ECM, and $\mathbf{Scc}(t) \in \mathbb{R}^{n,n}$ represents the matrix containing the non-negative cell-cell adhesion coefficients. Note that these matrices may have coefficients depending explicitly on time. We introduce the additional notation that $S_{c_i c_j} := (\mathbf{Scc})_{i,\,j}$ is the self-adhesion coefficient of sub-population i if $i = j$ and the cross-adhesion coefficient between sub-populations i and j if $j \neq i$. Furthermore $(\mathbf{Scv})i,i =: S_{c_i v}$. In the usual notation, the positive part of an expression is denoted by $(\cdot)^+ := \max\{0, \cdot\}$ and the factor $(1 - \rho(\mathbf{u}))^+$ models an inhibition of migration due to volume filling effects, see e.g. [28].

Cancer cells mutate and thus change membership from one cancer cell sub-population to another one. This gives rise to the structured-population model with n cancer cell sub-populations as considered here. The matrix $\mathbf{M}(\mathbf{u}(t, x)) \in \mathbb{R}^{n,n}$, multiplied by $\mathbf{c}$, represents the effect of mutations in (12). As in the case of the proliferation term, the factor $\mathbf{c}$ makes explicit that cells of sub-population i may mutate only if they already exist. Since mutations of cells of sub-population i correspond to a loss of cells in that sub-population and mutations of cells into cells of sub-population i correspond to a gain of cells in that sub-population, the diagonal elements of $\mathbf{M}$ must be non-positive and the off-diagonal elements of $\mathbf{M}$ must be non-negative. Furthermore, in order to ensure conservation of cell mass, we require that the column sums of $\mathbf{M}$ equal zero, i.e.

$$\sum_{i=1}^{n} M_{ij} = 0, \qquad \text{for} \quad j = 1, 2, \ldots, n. \tag{14}$$

Different additional structural conditions may apply to the matrix $\mathbf{M}$. For instance, if we assume that the cancer cell sub-populations are ordered such that mutations occur only towards sub-populations with a larger index, then matrix $\mathbf{M}$ is a lower triangular matrix, or, if we even assume that mutations occur only towards the sub-population with the next larger index, then $\mathbf{M}$ is even a lower bidiagonal matrix.

The evolution of the ECM density is governed by MDE-mediated matrix degradation as well as ECM remodelling. This is expressed as

$$\frac{\partial v}{\partial t} = -\gamma m v + \psi(t, \mathbf{u}), \tag{15}$$

where $\psi(t, \mathbf{u})$ represents the ECM remodelling law, and γ is the rate constant of ECM degradation due to the presence of MDEs. We require that $v = 0$ implies that $\psi(t, \mathbf{u}) \geq 0$ as this will ensure the non-negativity of the ECM density.

Finally, the evolution of the MDE concentration is determined by molecular diffusion of the enzymes, by natural decay, and by the release of MDEs by the cancer cell sub-populations into the tumour microenvironment. Hence we obtain

$$\frac{\partial m}{\partial t} = \nabla \cdot [D_3 \nabla m] + \alpha^{\top} \mathbf{c} - \lambda m. \tag{16}$$

In the above equation, D_3 is the positive MDE diffusion constant, $\boldsymbol{\alpha} \in \mathbb{R}^n$ is the non-negative vector of MDE release rates of the cancer cell sub-populations, and λ is the non-negative decay constant.

Model Application

Using the general formulation (12), (13a), (13b), (13c), (13d), (14), (15), and (16), we apply this framework to model the scenario of two cancer cell populations (phenotypes), c_1 and c_2, one of which may mutate into the other. We envisage a scenario where, as time develops, some of the cancer cells of type c_1 mutate to a more aggressive population c_2, leading to an increase of tumour malignancy [15]. In a different investigation, focused on the uPA system, [4] considered two cancer cells sub-populations within the context of a local-haptotaxis tumour cell movement model. The model for the two cancer cell populations, including mutation from one to the other, secretion of MDEs and interaction with the ECM is as follows:

$$\begin{aligned}
\frac{\partial c_1}{\partial t} &= \nabla \cdot [D_{11} \nabla c_1 - \mathcal{A}_1(u(t,\cdot)) c_1] + \mu_{11} c_1 (1 - c_1 - c_2 - v) - \delta_{c_1} F(t, v), \\
\frac{\partial c_2}{\partial t} &= \nabla \cdot [D_{12} \nabla c_2 - \mathcal{A}_2(u(t,\cdot)) c_2] + \mu_{12} c_2 (1 - c_1 - c_2 - v) - \delta_{c_1} F(t, v), \\
\frac{\partial v}{\partial t} &= -\gamma m v + \mu_2 (1 - c_1 - c_2 - v)^{+}, \\
\frac{\partial m}{\partial t} &= \nabla \cdot [D_3 \nabla m] + \alpha_1 c_1 + \alpha_2 c_2 - \lambda m,
\end{aligned} \tag{17}$$

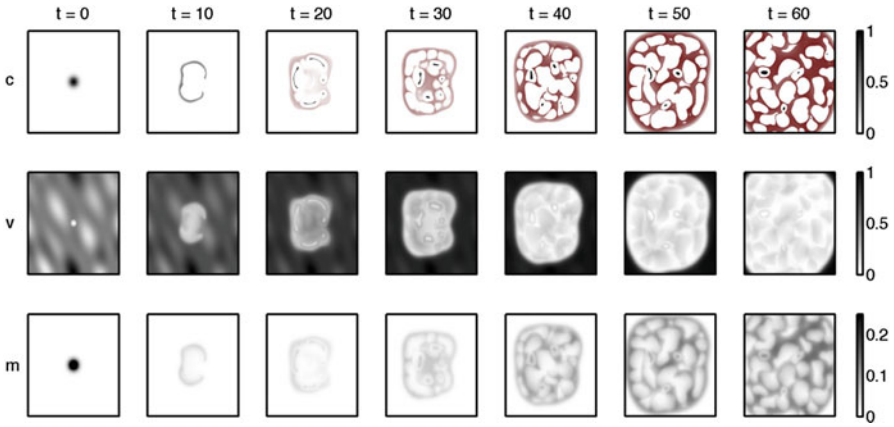

Fig. 6 Plots showing the cancer cell densities in the top row (black: $c1$, red: $c2$), ECM density v in the centre row, and the MDE concentration m in the bottom row at $t = 0$ (IC) and $t = 10, 20, \ldots, 60$ obtained from a simulation of model (17) with ECM reproduction rate $\mu_2 = 0.05$

with the conversion or mutation function

$$F(t, v) = H(t - t_{12}) \cdot H(v - v_{min}).$$

Here, H denotes the Heaviside function, t_{12} the time when the conversion from population 1 to population 2 starts and v_{min} is the minimal ECM density that is needed for a conversion to take place [4]. We assume that matrix remodelling process takes place while the locally available volume is not entirely occupied, i.e., as long as $1 - c_1 - c_2 - \mathrm{v} > 0$. Full details can be found in Domschke et al. [15].

Figure 6 shows the result of a simulation with the following parameter values (cf. [15, 19]). The cell-cell and cell-matrix adhesion parameters of both cancer cell sub-populations are kept constant and, from (13d), these are defined as

$$\mathbf{S_{cc}} = \begin{pmatrix} 0.5 & 0 \\ 0 & 0.3 \end{pmatrix} \qquad \mathbf{S_{cv}} = \begin{pmatrix} 0.3 & 0 \\ 0 & 0.5 \end{pmatrix}.$$

The remaining parameter values are as follows:

$$\gamma = 10 \qquad \mu_2 = 0.05 \qquad D_3 = 10^{-3}$$
$$\lambda = 0.5 \qquad R = 0.1$$

along with

$$c_1: \quad D_{11} = 10^{-4} \qquad \mu_{11} = 0.1 \qquad \alpha_1 = 0.1$$
$$c_2: \quad D_{12} = 10^{-4} \qquad \mu_{12} = 0.25 \qquad \alpha_2 = 0.1$$

and

$$\delta = 0.3 \qquad t_{12} = 10 \qquad v_{min} = 0.3.$$

From the plots in Fig. 6, we see that after time $t_{12} = 10$, the second population c_2 begins to emerges in the overall tumour cell density profile. Since the cell-cell cross-adhesion parameter $S_{c_1c_2}$ is zero, the two sub-populations do not mix. However, even though we have constant adhesive properties, the two cancer cell sub-populations form together with the (continuously remodelling) ECM a strongly heterogeneous pattern, reminiscent of invasion patterns observed clinically in lung and oesophageal cancers. A range of rich, heterogeneous spatio-temporal dynamics can be obtained by varying key parameters of the model such as the cell-cell and cell-matrix adhesive strengths in the matrices $\mathbf{S_{cc}}$ and $\mathbf{S_{cv}}$. Full details can be found in [15].

Discussion and Future Directions

In this chapter we have presented an overview of cancer modelling at various different important scales (intracellular, cellular and tissue) and focussing on key aspects (cf. hallmarks) of cancer – control of proliferation and differentiation, growth around blood vessels, local spread and invasion. While the modelling of GRNs (transcription factors) and cancer invasion was focussed on the relevant single scale (intracellular and tissue), the individual-based modelling in Sect. 3, with its inclusion of a basic cell-cycle in each cancer cell and an external oxygen field was genuinely multiscale in structure.

It is such multiscale modelling that holds out the best possibility for the development of optimal, individualised patient-based therapy in the future. Such a multiscale approach for modelling potential optimal treatment strategies (chemotherapy and radiotherapy) has already been explored by Powathil and co-workers [25, 41], while the very recent work of Franssen et al. [17] has, for the first time, developed a framework to model the metastatic spread of cancer from the primary tumour to secondary sites in the body. Since it is metastatic spread which is responsible for around 90% of deaths from cancer [22, 26], developing and clinically implementing predictive multiscale mathematical and computational models may well become an important part of cancer treatment in the years to come.

References

1. Alarcon, T., H. Byrne, and P. Maini. 2003. A cellular automaton model for tumour growth in inhomogeneous environment. *Journal of Theoretical Biology* 225: 257–274.
2. Alberts, B., D. Bray, K. Hopkin, A. Johnson, J. Lewis, M. Raff, K. Roberts, and P. Walter, eds. 2010. *Essential cell biology*. New York/London: Garland Publishing, Inc.
3. Alcaraz, J.L., M. Buscemi, X. Grabulosa, B. Trepat, R. Fabry, D. Farre, and D. Navajas. 2003. Microrheology of human lung epithelial cells measured by atomic force. *Biophysical Journal* 84: 2071–2079.
4. Andasari, V., A. Gerisch, G. Lolas, A. South, and M. Chaplain. 2011. Mathematical modeling of cancer cell invasion of tissue: Biological insight from mathematical analysis and computational simulation. *Journal of Mathematical Biology* 63 (1): 141–171.
5. Andasari, V., R. Roper, M.H. Swat, and M.A.J. Chaplain. 2012. Integrating intracellular dynamics using CompuCell3D and Bionetsolver: Applications to multiscale modelling of cancer cell growth and invasion. *PLoS ONE* 7 (3): e33726.
6. Anderson, A.R.A., and M.A.J. Chaplain. 1998. Continuous and discrete mathematical models of tumour-induced angiogenesis. *Bulletin of Mathematical Biology* 60: 857–899.
7. Armstrong, N.J., K.J. Painter, and J.A. Sherratt. 2006. A continuum approach to modelling cell–cell adhesion. *Journal of Theoretical Biology* 243 (1): 98–113.
8. Busenberg, S., and J.M. Mahaffy. 1985. Interaction of spatial diffusion and delays in models of genetic control by repression. *Journal of Mathematical Biology* 22: 313–333.
9. Chaplain, M.A.J., M. Ptashnyk, and M. Sturrock. 2015. Hopf bifurcation in a gene regulatory network model: Molecular movement causes oscillations. *Mathematical Models and Methods in Applied Sciences* 25 (6): 1179–1215.
10. Chu, Y.S., W.A. Thomas, O. Eder, E. Pincet, J.P. Thiery, and S. Dufour. 2004. Force measurements in e-cadherin–mediated cell doublets reveal rapid adhesion strengthened by actin cytoskeleton remodeling through rac and cdc42. *The Journal of Cell Biology* 167: 1183–1194.
11. Cytowski, M., and Z. Szymańska. 2014. Large scale parallel simulations of 3-d cell colony dynamics. *IEEE Computational Science and Engineering* 16 (5): 86–95.
12. ———. 2015. Enabling large scale individual-based modelling through high performance computing. *ITM Web of Conferences* 5: 00014.
13. ———. 2015. Large scale parallel simulations of 3-d cell colony dynamics. ii. coupling with continuous description of cellular environment. *IEEE Computational Science and Engineering* 17 (5): 44–48.
14. D'Antonio, G., P. Macklin, and L. Preziosi. 2013. An agent-based model for elasto-plastic mechanical interactions between cells, basement membrane and extracellular matrix. *Mathematical Biosciences and Engineering* 10: 75–101.
15. Domschke, P., D. Trucu, A. Gerisch, and M.A.J. Chaplain. 2014. Mathematical modelling of cancer invasion: Implications of cell adhesion variability for tumour infiltrative growth patterns. *Journal of Theoretical Biology* 361: 41–60.
16. Drasdo, D., and S. Höhme. 2005. A single-cell-based model of tumor growth in vitro: Monolayers and spheroids. *Physical Biology* 2: 133–147.
17. Franssen, L.C., T. Lorenzi, A.E.F. Burgess, and M.A.J. Chaplain. 2019. A mathematical framework for modelling the metastatic spread of cancer. *Bulletin of Mathematical Biology* 81: 1965–2010.
18. Galle, J., M. Loeffler, and D. Drasdo. 2005. Modelling the effect of deregulated proliferation and apoptosis on the growth dynamics of epithelial cell populations in vitro. *Biophysical Journal* 88: 62–75.
19. Gerisch, A., and M. Chaplain. 2008. Mathematical modelling of cancer cell invasion of tissue: Local and non-local models and the effect of adhesion. *Journal of Theoretical Biology* 250 (4): 684–704.

20. Glass, L., and S.A. Kauffman. 1970. Co-operative components, spatial localization and oscillatory cellular dynamics. *Journal of Theoretical Biology* 34: 219–237.
21. Goodwin, B.C. 1965. Oscillatory behaviour in enzymatic control processes. *Advances in Enzyme Regulation* 3: 425–428.
22. GP, G.P.G., and J. Massagué. 2006. Cancer metastasis: Building a framework. *Cell* 127 (4): 679–695.
23. Griffith, J.S. 1968. Mathematics of cellular control processes. i. negative feedback to one gene. *Journal of Theoretical Biology* 20: 202–208.
24. Gumbiner, B.M. 2005. Regulation of cadherin-mediated adhesion in morphogenesis. *Nature Reviews. Molecular Cell Biology* 6: 622–634.
25. Hamis, S., G.G. Powathil, and M.A.J. Chaplain. 2019. Blackboard to bedside: A mathematical modeling bottom-up approach toward personalized cancer treatments. *JCO Clinical Cancer Informatics* (3): 1–11. https://doi.org/10.1200/CCI.18.00068.
26. Hanahan, D., and R.A. Weinberg. 2000. The hallmarks of cancer. *Cell* 100: 57–70.
27. ———. 2011. Hallmarks of cancer: The next generation. *Cell* 144: 646–674.
28. Hillen, T., and K. Painter. 2001. Global existence for a parabolic chemotaxis model with prevention of overcrowding. *Advances in Applied Mathematics* 26 (4): 280–301.
29. Hirata, H., S. Yoshiura, T. Ohtsuka, Y. Bessho, T. Harada, K. Yoshikawa, and R. Kageyama. 2002. Oscillatory expression of the bHLH factor Hes1 regulated by a negative feedback loop. *Science* 298: 840–843.
30. Jagiella, N., B. Müller, M. Müller, I.E. Vignon-Clementel, and D. Drasdo. 2016. Inferring growth control mechanisms in growing multi-cellular spheroids of nsclc cells from spatial-temporal image data. *PLoS Computational Biology* 12 (2): e1004412.
31. Lachowicz, M., M. Parisot, and Z. Szymańska. 2016. Intracellular protein dynamics as a mathematical problem. *Discrete and Continuous Dynamical Systems. Series B* 21: 2551–2566.
32. Lahav, G., N. Rosenfeld, A. Sigal, N. Geva-Zatorsky, A.J. Levine, M.B. Elowitz, and U. Alon. 2004. Dynamics of the p53-Mdm2 feedback loop in individual cells. *Nature Genetics* 36: 147–150.
33. Macnamara, C.K., and M.A.J. Chaplain. 2016. Diffusion driven oscillations in gene regulatory networks. *Journal of Theoretical Biology* 407: 51–70.
34. ———. 2017. Spatio-temporal models of synthetic genetic oscillators. *Mathematical Biosciences and Engineering* 14: 249–262.
35. Macnamara, C.K., E.I. Mitchell, and M.A.J. Chaplain. 2019. Spatial-stochastic modelling of synthetic gene regulatory networks. *Journal of Theoretical Biology* 468: 27–44.
36. Mahaffy, J.M. 1988. Genetic control models with diffusion and delays. *Mathematical Biosciences* 90: 519–533.
37. Mahaffy, J.M., and C.V. Pao. 1984. Models of genetic control by repression with time delays and spatial effects. *Journal of Mathematical Biology* 20: 39–57.
38. Mahaffy, R.E., C.K. Shih, F.C. McKintosh, and J. Kaes. 2000. Scanning probe-based frequency-dependent microrheology of polymer gels and biological cells. *Physical Review Letters* 85: 880–883.
39. Miron-Mendoza, M., V. Koppaka, C. Zhou, and W.M. Petroll. 2013. Techniques for assessing 3-d cell-matrix mechanical interactions in vitro and in vivo. *Experimental Cell Research* 319: 2470–2480.
40. Näthke, I.S., L. Hinck, and W.J. Nelson. 1995. The cadherin/catenin complex: Connections to multiple cellular processes involved in cell adhesion, proliferation and morphogenesis. *Seminars in Developmental Biology* 6: 89–95.
41. Powathil, G.G., D.J. Adamson, and M.A.J. Chaplain. 2013. Towards predicting the response of a solid tumour to chemotherapy and radiotherapy treatments: Clinical insights from a computational model. *PLoS Computational Biology* 9 (7): e1003120. https://doi.org/10.1371/journal.pcbi.1003120.

42. Ramis-Conde, I., D. Drasdo, A.R.A. Anderson, and M.A.J. Chaplain. 2008. Modelling the the influence of the E-cadherin-β-catenin pathway in cancer cell invasion: A multi-scale approach. *Biophysical Journal* 95: 155–165.
43. Ritchie, T., W. Zhou, E. McKinstry, M. Hosch, Y. Zhang, I.S. Näthke, and J.F. Engelhardt. 2001. Developmental expression of catenins and associated proteins during submucosal gland morphogenesis in the airway. *Experimental Lung Research* 27: 121–141.
44. Schaller, G., Meyer-Hermann, M.: Multicellular tumor spheroid in an off-lattice Voronoi-Delaunay cell model. Physical Review E 71, 051910–1–051910–16 (2005)
45. Schlüter, D.K., I. Ramis-Conde, and M.A.J. Chaplain. 2012. Computational modeling of single cell migration: The leading role of extracellular matrix fibers. *Biophysical Journal* 103: 1141–1151.
46. ———. 2015. Multi-scale modelling of the dynamics of cell colonies: Insights into cell-adhesion forces and cancer invasion from in silico simulations. *Journal of the Royal Society, Interface* 12: 20141080.
47. Shymko, R.M., and L. Glass. 1974. Spatial switching in chemical reactions with heterogeneous catalysis. *The Journal of Chemical Physics* 60: 835–841.
48. Sturrock, M., A. Hellander, A. Matzavinos, and M.A.J. Chaplain. 2013. Spatial stochastic modelling of the hes1 gene regulatory network: Intrinsic noise can explain heterogeneity in embryonic stem cell differentiation. *Journal of the Royal Society, Interface* 10: 20120988.
49. Sturrock, M., A.J. Terry, D.P. Xirodimas, A.M. Thompson, and M.A.J. Chaplain. 2011. Spatio-temporal modelling of the Hes1 and p53-Mdm2 intracellular signalling pathways. *Journal of Theoretical Biology* 273: 15–31.
50. ———. 2012. Influence of the nuclear membrane, active transport, and cell shape on the Hes1 and p53-Mdm2 pathways: Insights from spatio-temporal modelling. *Bulletin of Mathematical Biology* 74: 1531–1579.
51. Szymańska, Z., M. Cytowski, E.I. Mitchell, C.K. Macnamara, and M.A.J. Chaplain. 2018. Computational modelling of cancer development and growth: Modelling at multiple scales and multiscale modelling. *Bulletin of Mathematical Biology* 80: 1366–1403.
52. Szymańska, Z., M. Parisot, and M. Lachowicz. 2014. Mathematical modeling of the intracellular protein dynamics: The importance of active transport along microtubules. *Journal of Theoretical Biology* 363: 118–128.
53. Weinberg, R.A. 2007. *The biology of cancer*. New York: Garland Science.
54. Zaman, M.H., L.M. Trapani, A.L. Sieminski, D. MacKellar, H. Gong, R.D. Kamm, A. Wells, D.A. Lauffenburger, and P. Matsudaira. 2006. Migration of tumor cells in 3d matrices is governed by matrix stiffness along with cell-matrix adhesion and proteolysis. *PNAS* 103: 10889–10894.